Monopole Core Instability and Alice Rings in Spinor Bose-Einstein Condensates

J. Ruostekoski[1] and J. R. Anglin[2]

[1]Department of Physical Sciences, University of Hertfordshire, Hatfield, Herts, AL10 9AB, United Kingdom
[2]Center for Ultracold Atoms, Massachusetts Institute of Technology,
77 Massachusetts Avenue, Cambridge, Massachusetts 02139, USA

We show how the length scale hierarchy, resulting from different interaction strengths in an optically trapped spin-1 ^{23}Na Bose-Einstein condensate, can lead to intriguing core deformations in singular topological defects. In particular, a point defect can be unstable with respect to the formation of a stable half-quantum vortex ring (an "Alice ring"), providing a realistic scheme to use dissipation as a sophisticated state engineering tool. We compute the threshold for stability of the point monopole, which is beyond the current experimental regime.

The rich order parameter space of multicomponent Bose-Einstein condensates (BECs) can admit truly 3D topological excitations [1–3], beyond the simple quantized vortices of single-component BECs. Such structures are of interest in a wide range of physical contexts, but dilute atomic BECs offer the unusual advantage that we can fully investigate, e.g., the short-range physics in topological defect cores, where the order parameter may explore a larger space than the usual ground state manifold. In this Letter we show how this can result in rich and surprising core structures, by demonstrating a spontaneous deformation of a singular point defect to an energetically stable half-quantum vortex ring. We evaluate the stable configurations for the parameters of current BEC experiments [4] and show how the half-quantum vortex ring could be prepared and easily observed using experimentally feasible techniques. We also present the energetic arguments behind the core deformations which apply to general multicomponent BECs.

We examine the recently presented case [3] of a defect analogous to the 't Hooft-Polyakov monopole [5], in an antiferromagnetic, or polar, spin-1 BEC [4]. We will show that it is only in the strongly antiferromagnetic regime, which is not attained in current experiments, that its stable core will be the spherically symmetric hedgehog, with a vanishing density, of Ref. [3]. In the weakly antiferromagnetic regime that currently holds, the wavelength at which the antiferromagnetic constraint may be violated is much larger than that at which the total density constraint fails. The stable defect core therefore extends to this larger size, and holds nonzero average spin instead of a density zero. The singular point defect itself deforms to a circle: a half-quantum vortex ring (Figs. 1 and 2), called an Alice ring by high energy physicists [6–8], which carries a topological charge similar to delocalized magnetic "Cheshire" charge [9]. This forms an interesting connection between ultracold atom experiments and elementary particle physics. It also shows that dissipation, often an obstacle in state engineering, can sometimes perform the intricate final step in producing an exotic object.

We consider the BEC of spin-1 atoms. In the absence of a magnetic trapping potential, the macroscopic BEC wave function is determined by a spinor wave function Ψ with three complex components [10]. The Hamiltonian density of the classical Gross-Pitaevskii (GP) mean-field theory for this system reads

$$\mathcal{H} = -\frac{\hbar^2}{2m}|\nabla\Psi|^2 + V\rho + \frac{c_0}{2}\rho^2 + \frac{c_2\rho^2}{2}|\langle\mathbf{F}\rangle|^2, \quad (1)$$

where $\mathbf{F}$ are the 3-by-3 Pauli spin matrices, $\langle\mathbf{F}\rangle = \Psi^\dagger \cdot \mathbf{F} \cdot \Psi/\rho$ denotes the average spin, $\rho = |\Psi|^2$ the total atom density, $c_0 \equiv 4\pi\hbar^2(2a_2 + a_0)/3m$, and $c_2 \equiv 4\pi\hbar^2(a_2 - a_0)/3m$, for a_F the two-body s-wave scattering length in the total spin F channel [10]. For ^{23}Na, $a_a \equiv (a_2 - a_0)/3 \simeq 2a_B$ and $a_s \equiv (2a_2 + a_0)/3 \simeq 50a_B$, indicating $c_2/c_0 \simeq 0.04$, where $a_B = 0.0529$ nm is the Bohr radius. Here V denotes the external potential, for an isotropic optical dipole trap with the frequency ω: $V(\mathbf{r}) = m\omega^2 r^2/2$. For ^{23}Na $c_2 > 0$, and the energy is minimized
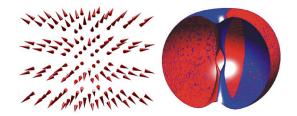

FIG. 1 (color online). The stable half-quantum vortex ring (Alice ring), when the energy of an initial spherically symmetric monopole was minimized by continuously deforming the field configuration. The asymptotic distribution of the spin quantization axis $\mathbf{d}(\mathbf{r})$ (left), for $r \gg \xi_a$, forms the radial hedgehog. For visualization purposes, the unoriented $\mathbf{d}(\mathbf{r})$ field is drawn by cones. We show the constant surface density plots (right) for $|\psi_1(\mathbf{r})|^2$ (red or light grey) and for $|\psi_{-1}(\mathbf{r})|^2$ (blue or dark grey), where the monopole core is deformed for $r \lesssim \xi_a$ with the two line vortices separating.
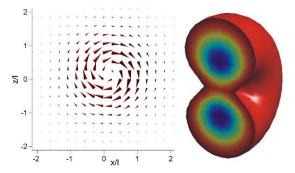
FIG. 2 (color online). The spin profile of the Alice ring displayed in Fig. 1. The spin expectation value $\langle \mathbf{F} \rangle$ (left) is nonvanishing along the half-quantum vortex ring core. The absolute value of the spin $|\langle \mathbf{F} \rangle|^2$ (right) between the isosurface sections ranges from $|\langle \mathbf{F} \rangle|^2 = 0.35$ at the boundary of the toroid (red) to $|\langle \mathbf{F} \rangle| = 1$ (purple or dark grey) at the center of the toroid. To display the isocaps of $|\langle \mathbf{F} \rangle|^2$ we have rotated the surface with respect to the spin field graph $\langle \mathbf{F} \rangle$ approximately $\pi/4$ counterclockwise along the z axis and cut the ring half.

by setting $\langle \mathbf{F} \rangle = \mathbf{0}$ throughout the BEC for the case of a uniform order parameter field. The zero average spin corresponds to the ground polar state, where we may determine all the degenerate states by means of the macroscopic BEC phase φ and a real unit vector $\mathbf{d(r)}$ defining the quantization axis of the spin. The BEC wave function then reads

$$\Psi = \begin{pmatrix} \psi_1 \\ \psi_0 \\ \psi_{-1} \end{pmatrix} = \frac{\sqrt{\rho}\, e^{i\varphi}}{\sqrt{2}} \begin{pmatrix} -d_x + i d_y \\ \sqrt{2}\, d_z \\ d_z + i d_y \end{pmatrix}. \quad (2)$$

As in the similar polar phase of superfluid ^{3}He-A [11–13], however, the states $(\mathbf{d}, \varphi)$ and $(-\mathbf{d}, \varphi + \pi)$ are identical [14]. The polar order parameter space, which may appear to be $S^1 \times S^2$, is actually factorized by the two-element discrete group Z_2. Consequently, we take the $\mathbf{d}$ field to define unoriented axes rather than vectors.

The spherically symmetric monopole Ψ_M is obtained from Eq. (2) by the radial hedgehog field $\mathbf{d(r)} = \hat{\mathbf{r}} \equiv (\sin\theta\cos\phi, \sin\theta\sin\phi, \cos\theta)$ [15,16], with $\varphi = 0$ and $\rho = \rho_M(r)$ minimizing the energy of the symmetric configuration [3]. This is singular at the origin indicating a point defect with $\rho(0) = 0$. Spinor component ψ_0 resembles a dark soliton and $\psi_{\pm 1}$ form perfectly overlapping, straight singly quantized vortex lines with opposite circulation, perpendicular to the phase kink plane. The topologically invariant winding number,

$$W = \frac{1}{8\pi} \int_{\partial\Omega} dS_i \epsilon_{ijk} \mathbf{d} \cdot \frac{\partial \mathbf{d}}{\partial x_j} \times \frac{\partial \mathbf{d}}{\partial x_k}, \quad (3)$$

is defined on any closed surface $\partial\Omega$ that encloses the origin. Because the sign of $\mathbf{d}$ is ambiguous, though, the sign of W is arbitrary. Moreover, because the $\mathbf{d}$ field is actually unoriented, the monopole point defect may be continuously deformed into a circular line defect, without changing W (on any surface enclosing the singular ring),

by puncturing a hole in the spherically symmetric core; see Fig. 3. To keep Ψ single valued on the disk bounded by the ring, the macroscopic phase φ must change by π around any loop that links the defect circle, while there is also a π disclination in $\mathbf{d}$ on the disk. We identify this structure as a half-quantum vortex line [11,12], forming a closed circular ring, also called an Alice ring [6–9]. To keep Ψ single valued on the ring itself, one can either have ρ vanish there or have $|\langle \mathbf{F} \rangle| = 1$ on the ring instead.

Thus, because of the ambiguity of the direction of $\mathbf{d}$ in the polar state, different core structures can be smoothly deformed into each other. The core stability is therefore solely determined by energetic considerations. Physically, the $\rho = 0$ ring evidently has higher energy than the $\rho = 0$ point, but energetic stability of the point defect against the Alice ring with $|\langle \mathbf{F} \rangle| = 1$ core is a nontrivial question. We may define two healing lengths $\xi_s \equiv (8\pi a_s \rho)^{-1/2}$ and $\xi_a \equiv (8\pi a_a \rho)^{-1/2}$ in Eq. (1). They describe the length scales over which ρ and $|\langle \mathbf{F} \rangle|$, respectively, tend to their bulk value when subjected to localized perturbations. (We can also say that ξ_s and ξ_a correspond to the excitation wavelengths below which density and spin fluctuations cease to be energetically suppressed.) Since at the defect core we may have either $\rho = 0$ or $|\langle \mathbf{F} \rangle| = 1$, ξ_s and ξ_a determine the core sizes in the two cases. We numerically demonstrate, by decreasing the ratio a_a/a_s, that the spherically symmetric monopole core with the total density suppression becomes unstable to formation of an energetically stable Alice ring with $|\langle \mathbf{F} \rangle| = 1$ core. We find the radial hedgehog to be unstable at $c_2/c_0 \lesssim 0.17$ in a linear stability analysis in bulk and in the mean-field theory in a trap, using an experimentally feasible set of parameters for ^{23}Na.

Before turning to the full nonlinear mean-field theory of the trapped BEC, we study the linear stability of the radial hedgehog in the homogeneous case. We expand the Hamiltonian (1), with $V = 0$, to second order around Ψ_M. Perturbations of the form

$$\delta\Psi = i\frac{\eta(r)}{\sqrt{2}} \begin{pmatrix} -C_1 + iC_2 \\ \sqrt{2}\, C_3 \\ C_1 + iC_2 \end{pmatrix} + i\frac{\mathbf{C} \cdot \hat{\mathbf{r}}}{\sqrt{2}} \mathsf{s}(r) \begin{pmatrix} -e^{-i\phi}\sin\theta \\ \sqrt{2}\cos\theta \\ e^{i\phi}\sin\theta \end{pmatrix} \quad (4)$$
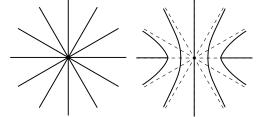

FIG. 3. Continuous deformation of the radial hedgehog into an Alice ring. Lines represent flow lines of the order parameter $\mathbf{d}$ field. We show planar sections of the monopole unperturbed (left) and deformed into an Alice ring (right). Note that the asymptotic behavior of $\mathbf{d}$ remains unchanged.

decouple from all others, for real C_j, η, and ς, if η and ς satisfy (here $X \equiv c_2/c_0$ and $\bar{\rho} \equiv \rho_M(r)/\rho_0$, where ρ_0 denotes the constant asymptotic value of the density)

$$\lambda \varsigma = -\frac{1}{2r^2}(r^2 \varsigma')' + \frac{3}{r^2}\varsigma + [(\bar{\rho}-1)\varsigma - 2X\bar{\rho}\eta]\frac{1}{\xi_s^2},$$

$$\lambda \eta = -\frac{1}{2r^2}(r^2 \eta')' + [\bar{\rho}(1+2X) - 1]\frac{\eta}{\xi_s^2} - \frac{\varsigma}{r^2} \quad (5)$$

for some real eigenvalue λ. For small $C = |\mathbf{C}|$, the change in free energy due to this perturbation in Ψ will be $\delta E = \lambda C^2 m/\hbar^2$. Numerical solution shows [17] that there exists one negative λ, hence three degenerate instabilities proportional to C_i, when $c_2/c_0 \lesssim 0.17$. We can show that no other instabilities exist in bulk, so for $c_2/c_0 \gtrsim 0.17$ the point defect is stable. Since the perturbation (4) gives

$$\langle \mathbf{F} \rangle = \frac{2\mathbf{C} \times \hat{\mathbf{r}}\sqrt{\rho_M}\,\eta}{\rho_M + C^2 \eta^2}, \quad (6)$$

where $\langle \mathbf{F} \rangle$ is with respect to the state $\Psi_M + \delta\Psi$, we have $|\langle \mathbf{F} \rangle| = 1$ on a circle in the plane through the origin perpendicular to $\mathbf{C}$, at radius r_*, such that $\rho_M(r_*) = [C\eta(r_*)]^2$. The form of $\rho_M(r)$ (rising monotonically from 0 to ρ_0) and η (decreasing monotonically to zero as $r \to \infty$) ensures that r_* grows monotonically with C. As a result, a randomly oriented Alice ring will form spontaneously from the symmetric monopole, as C grows from zero by relaxation, for $c_2/c_0 \lesssim 0.17$.

In the full 3D classical mean-field theory of the spin-1 monopole in an isotropic trap, we minimized the energy by evolving the GP equations,

$$i\hbar \frac{\partial \Psi}{\partial t} = \left(-\frac{\hbar^2}{2m}\nabla^2 + V + c_0\rho\right)\Psi + c_2\rho\langle \mathbf{F} \rangle \cdot \mathbf{F} \cdot \Psi,$$

$$(7)$$

in imaginary time. The initial state was an approximate spherically symmetric monopole solution with a point core, embedded in a Thomas-Fermi density profile. The integration was performed on a spatial grid of 128^3 points using the split-step method. At every time step we normalized the wave function to fix the total atom number. The numerical simulations were fully 3D without imposing any symmetry on Ψ as it relaxed.

We varied the relative strength of the two interaction coefficients c_0 and c_2, as well as the total atom number N. The dynamics depends on the dimensionless interaction strengths $c_0' = 4\pi N a_s/l$ and $c_2' = 4\pi N a_a/l$, where $l \equiv [\hbar/(m\omega)]^{1/2}$. Hence, for a given atom with fixed values of scattering lengths, the results are unchanged for any scaling of length and time, which does not change $N^2\omega$. In optical dipole trap experiments on ^{23}Na BECs, a wide range of aspect ratios and trapping strengths have been demonstrated, with the typical values of l/a_s varying between 500 and 4000 [4].

For small values of c_2/c_0, the point core deformed into a half-quantum vortex ring. With the initial radial hedgehog at the trap center we found vortex ring configurations

as local energetic minima, with the size of the ring approximately determined by ξ_a. In Figs. 1 and 2 we display such results using the parameters of the spin-1 ^{23}Na with $c_2/c_0 = 0.04$ and $c_0' = 2 \times 10^4$. With the trapping frequency $\omega = 2\pi \times 10$ Hz, this corresponds to $N \simeq 4 \times 10^6$ atoms. In the initial state of the radial hedgehog, the components $\psi_{\pm 1}$ form two oppositely circulating vortex lines with perfectly overlapping density profiles. Because of dissipation, the two vortices in $\psi_{\pm 1}$ separated near the trap center, forming an Alice ring. Note that this corresponds to the growth of the perturbation C_2 in Eq. (4). The numerical noise in this example effectively seeded the instability C_2 yielding

$$\psi_{\pm 1}^{(M)} + \delta\psi_{\pm 1} \propto \frac{\sqrt{\rho_M}}{r}\left[\left(\mp x - \frac{C_2 r\eta}{\sqrt{\rho_M}}\right) + iy\right]. \quad (8)$$

Since $r\eta/\sqrt{\rho_M}$ is constant at the origin, but vanishes as $r \to \infty$, this means that near the center the two vortices in $\psi_{\pm 1}$ separate in the xz plane. Growth of C_1 involves a similar separation in the yz plane. One can clearly see the π winding of the macroscopic phase around closed loops threading the Alice ring in Eq. (8).

With some initial parameters we also observed the radial hedgehog evolving to an Alice ring with the vortex cores in $\psi_{\pm 1}$ expanding, but not separating, while the phase kink in ψ_0 no longer maintained a vanishing density at the center. This clearly represents the growth of the perturbation C_3 in Eq. (4), since the term proportional to $\varsigma(r)$ is simply a perturbation in the macroscopic phase φ of Eq. (2). In the general case of a symmetric initial monopole, the spherical symmetry spontaneously breaks as the system deforms due to dissipation and the resulting ring has an arbitrary orientation.

It is easy to see that the Alice ring in bulk must stabilize at some finite value of the radius, because the amount of energetically costly nonzero $\langle \mathbf{F} \rangle$ rises as the ring grows. This was also true in a trap for small enough rings. However, with smaller atom numbers, $c_0' \lesssim 10^4$ for ^{23}Na, a larger ring resulted, which was destabilized by the inhomogeneous density profile: the two vortex lines in $\psi_{\pm 1}$ completely detached and left the atomic cloud in opposite directions.

The half-quantum vortex ring, shown in Figs. 1 and 2, was still unstable with respect to drifting out of the atomic cloud as a unit if initially displaced from the trap center. This is because of the reduced order parameter bending energy at lower atom densities. However, we successfully stabilized the Alice ring by creating a local density minimum at the trap center, by adding to the harmonic trapping potential the optical potential V_L, simulating two orthogonal blue-detuned focused Gaussian laser beams: $V_L = V_1 \exp[-2(x^2 + y^2)/w^2] + V_2 \exp[-2(x^2 + z^2)/w^2]$. We note that the Alice ring can always be made long-living on experimental time scales even without the stabilizing field, since the drift time

should increase with the BEC size, while the ring formation time should decrease.

We also investigated the onset of the point defect core instability by varying c_2' for a given $c_0' = 2 \times 10^4$. We found the symmetric monopole to be unstable for $c_2/c_0 \lesssim 0.17$, in a good agreement with the linear stability analysis in bulk. The precise value of the threshold is very difficult to determine in a trap, since the convergence in the simulations is particularly slow close to the threshold. In the case of very long runs, numerical noise also eventually displaces the monopole so that it starts drifting out of the atomic cloud. For smaller values of c_2', representing unstable Alice rings which break apart due to the inhomogeneous density, the instability of the point defect occurred with much larger values of c_2/c_0, when the trap length scale became comparable to the polar healing length $l \sim \xi_a$, emphasizing the nontrivial nature of the finite size effects.

In the experimental preparation of an Alice ring by relaxation, it is helpful to note that defects and textures in multicomponent BECs may generally be viewed as combinations of vortex lines, rings, and phase kinks [18]. As we already noted, the radial hedgehog has an especially simple structure of vortex lines and phase kinks which have been experimentally created in individual atomic BEC components, e.g., by means of localized laser fields, which are rapidly swept around the trap during a Raman transition [19–21]. The spherically symmetric monopole could similarly be created, by a sequence of Raman pulses, in a straightforward generalization of the pulse sequences proposed in Ref. [18]. Dissipation plays a crucial role in the state engineering process and will then perform the final step of generating a stable Alice ring by spontaneously breaking the spherical symmetry. The stable radius ξ_a of the Alice ring may easily extend over several microns, making the core quite observable, possibly even without ballistic expansion.

The relaxation time of other defects, such as simple vortex rings in a single-component BEC [20] via shrinking, indicate that the point defect core deformation could be rapid on experimental time scales. We may obtain a rough estimate for the initial deformation rate due to dissipation by thermal atoms from $\gamma \hbar \omega_R/(k_B T)$, where $\gamma = 8\pi a_s^2 \rho_{\mathrm{nc}} \hbar k/m$ denotes the Boltzmann collision rate of thermal atoms with density ρ_{nc} and ω_R is the unstable Bogoliubov mode frequency. Using the same values as before with $\rho_{\mathrm{nc}} \sim 10^{13}$ cm^{-3} and $T \sim 100$ nK indicates that the Alice ring could form in a few seconds allowing a real-time monitoring of the deformation.

We can summarize our results in basic terms. In ^{23}Na BECs the weakness of the antiferromagnetic energy ($a_s \gg a_a$), topology, and the gradient energy of the order parameter may conspire to favor nonvanishing spin values, even for $a_a > 0$: It is energetically more favorable to violate the antiferromagnetic constraint than to force the

superfluid density to vanish. As a result, a monopole core deforms to a ring and exhibits a nonvanishing spin expectation value and a nonzero superfluid density. In other words, the strong order parameter bending energy close to the singular defect mixes the polar and the ferromagnetic phases of the spinor BEC, rather than forcing the total superfluid density to zero at the singularity. Because of the length scale hierarchy, the stable size of the defect core will then be determined by ξ_a instead of the much smaller ξ_s. And the creation of this intricate Alice ring structure will occur spontaneously, from the much simpler symmetric monopole, by relaxation alone.

While the motion and interaction of point defects was analyzed in Ref. [3], the dynamics of Alice rings remains a question for future theoretical and experimental study. So does the possible metastability of Alice rings for $c_2 \gtrsim 0.17c_0$. Topological defects in spinor BECs promise a rich phenomenology, which current experimental techniques will allow us to explore.

---

[1] C. M. Savage and J. Ruostekoski, Phys. Rev. Lett. **91**, 010403 (2003), and references therein.

[2] M. A. Metlitski and A. R. Zhitnitsky, cond-mat/0307559.

[3] H. T. C. Stoof et al., Phys. Rev. Lett. **87**, 120407 (2001).

[4] A. E. Leanhardt et al., Phys. Rev. Lett. **90**, 140403 (2003).

[5] G. 't Hooft, Nucl. Phys. **B79**, 276 (1974); A. M. Polyakov, JETP Lett. **20**, 194 (1974).

[6] A. S. Schwarz, Nucl. Phys. **B208**, 141 (1982).

[7] F. A. Bais and P. John, Int. J. Mod. Phys. A **10**, 3241 (1995).

[8] J. Striet and F. A. Bais, hep-th/0304189.

[9] M. Alford et al., Nucl. Phys. **B349**, 414 (1991).

[10] T.-L. Ho, Phys. Rev. Lett. **81**, 742 (1998); T. Ohmi and K. Machida, J. Phys. Soc. Jpn. **67**, 1822 (1998).

[11] D. Vollhardt and P. Wölfle, *The Superfluid Phases of Helium 3* (Taylor and Francis, London, 1990).

[12] G. E. Volovik, *The Universe in a Helium Droplet* (Oxford University Press, Oxford, 2003).

[13] G. E. Volovik and V. P. Mineev, Sov. Phys. JETP **45**, 1186 (1977) [Zh. Eksp. Teor. Fiz. **72**, 2256 (1977)].

[14] U. Leonhardt and G. E. Volovik, JETP Lett. **72**, 46 (2000).

[15] For an analogous 2D hedgehog structure, see Th. Busch and J. R. Anglin, Phys. Rev. A **60**, R2669 (1999).

[16] For Dirac monopoles, see C. M. Savage and J. Ruostekoski, Phys. Rev. A **68**, 043604 (2003).

[17] J. R. Anglin and J. Ruostekoski (to be published).

[18] J. Ruostekoski and J. R. Anglin, Phys. Rev. Lett. **86**, 3934 (2001).

[19] M. R. Matthews et al., Phys. Rev. Lett. **83**, 3358 (1999).

[20] B. P. Anderson et al., Phys. Rev. Lett. **86**, 2926 (2001).

[21] For alternative creation methods, see J. Ruostekoski, Phys. Rev. A **61**, 041603 (2000), and references therein.